

## Research Article

## Film Cooling Characteristics of a Single Round Hole at Various Streamwise Injection Angles

P.Venkata Vara Prasad<sup>Å</sup>, Surisetty Naga Kishore<sup>Å\*</sup> and T.Venkateswara Rao<sup>Å</sup>

<sup>Å</sup>Department of Mechanical Engineering, DBS Institute of Technology, Kavali-524201, India.

Accepted 30 March 2014, Available online 01 April 2014, Vol.4, No.2 (April 2014)

### Abstract

Film cooling is the method used to protect the surface exposed to high temperature flows such as those that exist in gas turbines. It involves the injection of secondary fluid that covers the surface to be protected. In this study, film cooling effectiveness was investigated numerically on a cylindrical hole with a stream wise angle of 30°, 60° and 90° in a flat plate test facility with a zero pressure gradient. The short but engine representative hole length ( $L/D=4$ ) is constant for all the geometries. The blowing ratio ranges from 0.33 to 1.67. The current results are compared with the experimental results obtained by Yuen and Martinez-Botas and the effects of variations in injection angle are described.

**Keywords:** Blowing ratio ( $M$ ), Injection Angle, Velocity, Temperature, Fluent, Heat transfer coefficient,

### 1. Introduction

A common problem in heat transfer arises from the need to protect solid surface exposed to high temperature environment. One method of providing this protection is to introduce a secondary fluid into the boundary layer next to the solid surface. This process includes Ablation, Transpiration and film cooling.

Ablation involves the use of a coating or heat shield that decomposes to gas that enters the boundary layer. A disadvantage of this method is that the coating is non-renewable, so the method is restricted to high heat fluxes of short duration, such as re-entering space vehicles. In transpiration, the surface is porous and a secondary fluid enters the boundary layers through the porous wall. A disadvantage to this method is that porous materials lack the high strength needed for certain applications such as turbine rotors. The difference between film cooling and the first two methods mentioned above (Ablation and Transpiration) is that in film cooling, it is not only the region in the immediate vicinity of injection but also the region downstream of injection that is being protected.

There are two significant Variables in film cooling are Geometry and flow field. In 2-dimensional film cooling, the external flow field is 2-dimensional and the secondary fluid is introduced uniformly across the span. But in 3-D film cooling the geometry has significant effect. Injection is not uniform across the span, but instead is through discrete holes at isolated location. This can result in the secondary fluid blown off of the surface as well as the mainstream flow going between the coolant and the wall. Yuen and Martinez-Botas (2003a) were studied film cooling effectiveness of cylindrical hole with a stream

wise angle of 30°, 60° and 90° in a flat plate test facility with a zero pressure gradient. A hole length of  $L/D=4$  was used, the free-stream Reynolds number based on the free-stream velocity and hole diameter was 8563, and the blowing ratio was varied from 0.33 to 2 (Yuen *et al*, 2003a). Yuen and Martinez-Botas (2003b) were used liquid-crystal thermography to experimentally measure heat transfer coefficients downstream of a cylindrical hole at an angle of 30°, 60°, and 90°. Again, a hole length of  $L/D=4$  was used, the free-stream Reynolds number based on the free-stream velocity and the hole diameter was 8563, and the blowing ratio was varied from 0.33 to 2 (Yuen *et al*, 2003b). D. K. Walters and J. H. Leylek presented for a three-dimensional discrete-jet in crossflow problem typical of a realistic film-cooling application in gas turbines (D. K. Walters *et al*, 1997). Brown and Saluja (1978) calculated film cooling effectiveness on a flat plate in a wind tunnel. Tests were done using a single cylindrical hole and, in three cases, a row of cylindrical holes. The holes were inclined at an angle of 30° from the test surface, and pitch-to-diameter ratios of 8.0, 5.33, and 2.67 were used. It was found that as the pitch was decreased, the laterally-averaged effectiveness increased. Also, the maximum effectiveness was found to occur at a blowing ratio of around 0.5 for all cases (Saluja *et al*, 1978). R. S. Bunker *et al*. studied on experimental design to obtain detailed radial heat transfer coefficient distributions applicable to the cooling of disk-cavity regions of gas turbines. An experimental setup was designed to obtain local heat transfer data on both the rotating and stationary surfaces of a parallel geometry disk-cavity system (R. S. Bunker *et al*, 1992a). D. E. Metzger *et al*. presented on detail radial distributions of rotor heat transfer coefficients for three basic disk-cavity

\*Corresponding author: Surisetty Naga Kishore

geometries applicable to gas turbines. Cooling air was introduced into the disk cavity via a single circular jet mounted perpendicularly into the stator at one of the three radial locations: 0.4, 0.6, or 0.8 times the rotor radius (Metzger *et al*, 1992b). D. L. Schmidt *et al*. Studied experimentally on Film cooling effectiveness in a flat plate test facility with zero pressure gradient using a single row of inclined holes, which injected high-density, cryogenically cooled air (D. L. Schmidt *et al*, 1996). G E. Andrews *et al*. were described experimental techniques for the determination of the overall heat transfer in a metal plate with a large number of coolant holes drilled at 90 deg. The results were compared with conventional short-tube internal heat transfer measurements and shown to involve much higher heat transfer rates and this mainly resulted from the additional hole approach flow heat transfer (G. E. Andrews *et al*, 1986). D. Crabb *et al*. confirmed and measured the double-vortex characteristics of the downstream flow and demonstrate that this was associated with fluid emanating from the jet. The velocity maximum observed further from the wall than the double vortex was shown to correspond to free stream fluid accelerated by the pressure field (D. Crabb *et al*,1981). Rhee *et al*. (2003) conducted an experimental study to investigate effectiveness for one, two, and three rows of four different types of film cooling holes: two sizes of circular holes, a rectangular hole, and a rectangular hole with an expanded exit (Rhee *et al*, 2003).The numerical simulation process coupled ANSYS CFX software for the fluid flow, ANSYS Mechanical software for the structural response of the blade, and the 1-D thermal and fluid flow simulation package Flowmaster2. This set of simulation tools provided an efficient virtual prototype that was used to assess the performance of the turbine blade under actual operating conditions (Ansys Manual).

In this study, Film cooling effectiveness is studied numerically on cylindrical holes with steam wise angle of 30°, 60° and 90° with blowing ratio ranging from 0.33 to 1.67. The direction of cross flow is from left to right, the origin of axial distance x/D commences from the centre of the cooling hole and temperatures are decreased on two dimensional surface with increasing of blowing ratio.

## 2. Film Cooling

One of the widely used blade cooling technique is film cooling. In film cooling system a small amount of cooling air is bled from the main-engine compressor at outlet condition and introduced into the turbine-rotor disk at a point near the shaft axis as shown in Fig 1.6.

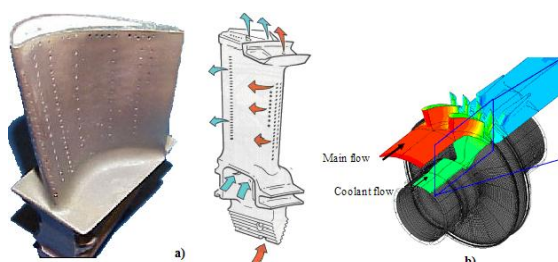


**Figure1:** (a) Film cooling hole in turbine blade and (b) simulation of coolant flow in turbine rotor

The coolant is then pumped out through the hollow disk passages and blades and is discharged from the blade tip which is shown in Fig 1.7. The cooling air then mixes with the main-engine gas flow and passes into the jet nozzle. The coolant temperature entering the blade base is equal to the main engine compressor-outlet temperature plus allowances for heat transfer and additional compression as the coolant passes through the disks. The coolant flow is regulated by a throttling valve in the bleed line.

This air provides a thin, cooler, insulating film along the external surface of the turbine blade as shown in Fig 2, due to which the method is called film cooling. That film provides protection and thus increases the life of the blade.

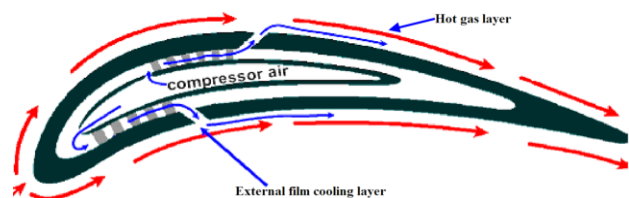


**Figure 2:** The schematic of film cooling of gas turbine blade

Unfortunately, this cold film protection comes at the expense of thrust. The source of the cold coolant air is bled-off air from the last stage of the compressor section. This high pressure air bypasses the combustor section of the engine and is maintained at much lower temperatures than the core turbine flow. This bled-off air, however, is removed from the core mass flow and subtracts from the overall thrust of the engine. Obviously, the engine designer wants to minimize the amount of bled-off air required to cool the blade. From this, it is apparent that a good understanding of not only how film cooling schemes affect heat transfer is needed, but also an understanding of what parameters control the level of effectiveness provided is needed. Also the cooling performance can be influenced by a variety of parameters, i.e. the blade and discharge geometry, injection angle, blowing ratio, free stream turbulence; reliable prediction methods can be of vital interest for turbine-blade designers.

## 3 Design Parameters

### 3.1. Heat Transfer Coefficient

In present paper we consider that the coolant air is being injected from the bottom of the plate surface as shown in below fig. Now in addition to the mainstream flow, we have a secondary flow. We have 3 different temperatures to consider  $T_\infty$ ,  $T_w$  and  $T_f$ . Coolant temperature  $T_f$  don't address the problem completely as the temperature difference term in equation (1) needs the local temperature.

Local heat transfer flux is represented by

$$q''_0 = h_0(T_\infty - T_w) \tag{1}$$

Where  $h_0$  is the transfer coefficient on the surface with a

wall temperature  $T_w$  and on coming hot mainstream gas temperature  $T_\infty$ . The heat load changes upon the injection of coolant over the blade surface and is represented as

$$q_0 = h(T_\infty - T_w) \tag{2}$$

where,  $h$  is the heat transfer coefficient on the surface with film cooling and  $T_f$  is the film temperature.

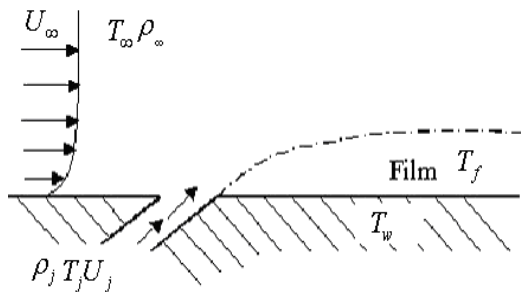


**Figure3:** Protective film layer made by coolant injection

In general the injection of film cooling changes the fluid flow profile around the blade and usually increases the heat transfer coefficient. This increase in  $h$  is undesirable as it promotes heat transfer from the hot free stream flow and good designs of film cooling should attempt to minimize this increase. Obviously, an understanding of exactly how film coolant schemes affect the heat transfer coefficient is important. With the introduction of film cooling has the effect of increasing  $h$  slightly, the technique's advantages is realized by large decrease of the wall temperature,  $T_w$ .

### 3.2 Film cooling Effectiveness

The term effectiveness ( $\eta$ ) referred to the maximum value. if the film temperature is equal to the coolant temperature it could be taken as 1. The theoretical scenario implies that the film is 100% effective. In contrast, the film effectiveness is worst ( $\eta=0$ ) when the temperature of the film is equal to the main, hot, stream.

$$\eta = \frac{T_\infty - T_{aw}}{T_\infty - T_j}$$

### 3.3. Film cooling parameters

This study is a computational investigation of parameters affecting the film cooling effectiveness. In general, effectiveness's ( $\eta$ ) are functions of many parameters in an engine environment. The most influential parameters can be grouped into two categories, Aerodynamics and Geometry. Specifically effectiveness's ( $\eta$ ) are functions of,

#### 3.3.1. Cooling Geometry

- Local free stream Mach number,  $Ma$
- Downstream location,
- Coolant scheme geometry (hole length, hole spacing, blowing angle, etc.)

#### 3.3.2. Aerodynamics

- Film Cooling Blowing Ratio,  $M$ ,
- Film cooling Density Ratio,  $DR$ ,
- Free stream Turbulence,  $TL$

#### CFD for Film Cooling

By introducing a coolant fluid, film cooling is used to provide heat protection for wall surfaces under high thermal load, such as turbine blades. A lot of experimental work in film cooling has been done in the past forty years. But since the film cooling problem is very complex, it has been found that it is really difficult to achieve a universal equation to predict the film cooling effectiveness according to the experimental results. Thus there is importance in performing a numerical study of film cooling to contribute to added understanding of the film cooling effectiveness. CFD provides the opportunity to investigate the full developing flow field in detail.

CFD solvers are usually based on the finite volume method.

- Domain is discretized into a finite set of control volumes or cells.
- General conservation (transport) equation for mass, momentum, energy etc; are discretized into algebraic equation is shown in below fig.4
- All equations are solved to render flow field.

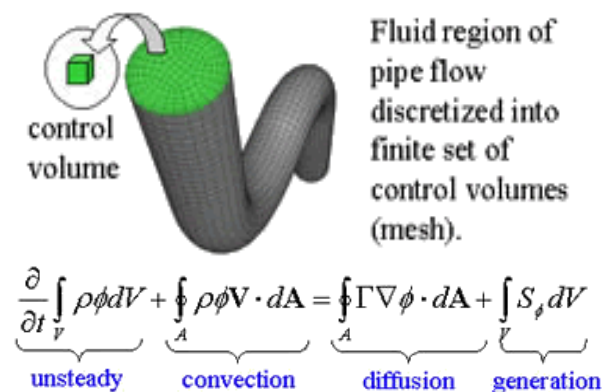


**Fig 4:** General conservation (transport) equation for mass, momentum, energy are discretized into algebraic equation

Analysis begins with a mathematical model of a physical problem

- Conservation of matter, momentum, and energy must be satisfied throughout the region of interest.
- Fluid properties are modeled empirically.
- Simplifying assumptions are made in order to make the problem tractable e.g., steady-state, incompressible, in viscid, two-dimensional.
- Provide appropriate initial and/or boundary conditions for the problem.

CFD applies numerical methods (called discretization) to develop approximations of the governing equations of fluid mechanics and the fluid region to be studied.

- Governing differential equations become algebraic.
- The collection of cells is called the grid or mesh.

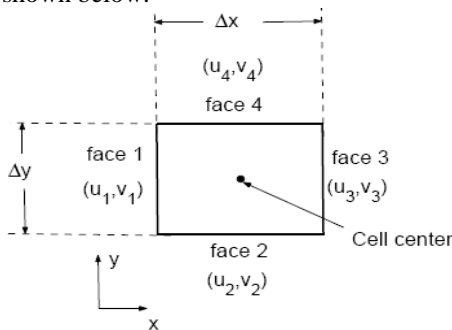
- The set of approximating equations are solved numerically (on a computer) for the flow field variables at each node or cell.
- System of equations is solved simultaneously to provide solution.

### 3.4 Discretization using the Finite-Volume Method

In the finite-volume method, a quadrilateral is commonly referred to as a cell and a grid point as a node. In 2D, it could also have triangular cells. In 3D, cells are usually hexahedral, tetrahedral or Prisms. In finite volume method approach, the integral form of the conservation equation is applied to the control volume defined by a cell to get the discrete equations for the cell. The integral form of the continuity equation for steady incompressible flow is

$$\int_S \mathbf{V} \cdot \hat{\mathbf{n}} ds \quad (3)$$

The integration is over the surface S of the control volume and  $\hat{\mathbf{n}}$  is the outward normal at the surface. Physically, this equation means that the net volume flow into the control volume is zero. Consider the rectangular cell shown below.



The velocity at face i is taken to be  $\mathbf{V}_i = u_i \hat{i} + v_i \hat{j}$ . Applying the mass conservation equation (5) to the control volume defined by the cell gives.

$$-u_1 \Delta y - v_2 \Delta x + u_3 \Delta y + v_4 \Delta x = 0 \quad (4)$$

This is the discrete form of the continuity equation for the cell. It is equivalent to summing up the net mass flow into the control volume and setting it to zero. So it ensures that the net mass flow into the cell is zero i.e. the mass is conserved for the cell. Usually the value at the cell centers is stored. The face values  $u_1, v_2, u_3, v_4$  are obtained by suitably interpolating the cell-center values at adjacent cells.

Similarly, discrete equations for the conservation of momentum and energy for the cell can be obtained. These ideas can be readily extended to any general cell shape in 2D or 3D and any conservation equation.

### 3.5 Basic Steps of CFD Analysis

Preprocessing involves generation of the geometry and identification of the domain to be modeled followed by discretization of it into a number of small cells. Depending

on the type of problem, suitable transport equations for mass, momentum and energy are considered and other equations governing the physical models like turbulence, combustion, radiation, multiphase etc. are solved over these cells on providing appropriate solver settings. Proper material properties, boundary conditions and initial conditions shall be defined over the discretized model and is vital in obtaining accurate results. Post processing is the final stage in which the results obtained are validated with simple calculations and experimental data if available. In case the results are not satisfactory revisions to the model are considered and the cycle is repeated until satisfactory results are achieved.

### 3.6 Introduction to Fluent

Fluent is the world's largest provider of commercial computational fluid dynamics (CFD) software and services. FLUENT is a state-of-the-art computer program for modeling fluid flow and heat transfer in complex geometries. FLUENT provides complete mesh flexibility, including the ability to solve flow problems using unstructured meshes that can be generated about complex geometries with relative ease. Supported mesh types include 2D triangular/Quadrilateral, 3D tetrahedral/hexahedral/ pyramid/ wedge and mixed (hybrid) meshes. FLUENT also allows refining or coarsening the grid based on the flow solution.

Once a mesh has been read into FLUENT, all remaining operations are performed within FLUENT. These include setting boundary conditions, defining fluid properties, executing the solution, refining the mesh, and viewing and post processing the results.

The FLUENT serial solver manages file input and output, data storage, and flow field calculations using a single solver process on a single computer. FLUENT also uses a utility called cortex that manages FLUENT's user interface and basic graphical functions. FLUENT's parallel solver allows to compute a solution using multiple processes that may be executing on the same computer, or on different computers in a network.

FLUENT is ideally suited for incompressible and compressible fluid-flow simulations in complex geometry. FLUENT Inc. also offers other solvers that address different flow regimes and incorporate alternative physical models.

### 3.7 Geometry of the Computation Domain Boundary conditions

At the main inlet, a velocity-inlet boundary condition was specified with X-velocity equal to 13m/s and all other components equal to zero. The temperature was given as 293.16 K. The turbulence intensity and hydraulic diameter (which is used to determine turbulence length scales) was specified as 2.7% and 0.173165 m, respectively.

At the coolant inlet, a velocity-inlet boundary condition was specified with Y- velocity equal to the values given in below table and all other components equal to zero. The temperature was given as 313.15 K. the turbulence intensity and hydraulic diameter were specified

as 3% and 0.15 m, respectively.

Case Number	Blowing Ratio	Velocity(m/s)
1	0.33	0.01256
2	0.5	0.01903
3	0.67	0.0255
4	1	0.0381
5	1.33	0.0506
6	1.67	0.063

The boundary conditions specified above is same for the stream wise angles 30°,60° and 90°

At the outlet, a pressure-outlet boundary condition was specified with gage pressure equal to 0 (given as absolute pressure of 101,325 Pa)

#### 4. Meshes

The meshes for the three cases were created using ICEM-CFD. A Picture of 1,80,384 hexahedral cell mesh for the geometry with three stream wise angles 30°,60° and 90° is shown in figure.

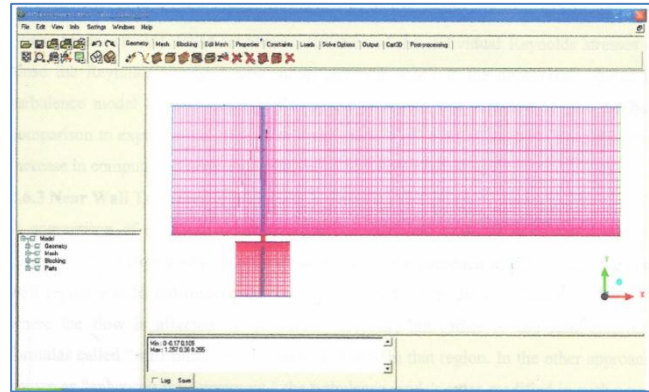


Fig 7: Mesh for 90 degree stream wise injection angle

#### Solver

For the Present problem solution was obtained by using the 3D segregated solver in FLUENT

#### Overview of Turbulence Models

In this study solutions were obtained using three different types of turbulence models and compared to experimental results. The three models were k-ε, k-U), and the Reynolds Stress Model (RSM). RSM involves calculation of the individual Reynolds stresses to close the Reynolds-averaged momentum equation. RSM is the appropriate choice of turbulence model for non-isotropic flows, and was therefore expected to give the best comparison to experimental data. A downside to using the RSM model is the significant increase in computation time required to get a converged solution.

#### Near Wall Treatments

A comparison of solutions obtained using two different types of near wall treatment (using RSM) to experimental data was also made. One approach used to model the near wall region was to not resolve the flow in the region immediately adjacent to the wall where the flow is affected by molecular viscosity, but rather to use semi-empirical formulas called wall functions to model the flow in that region. In the other approach, known as enhanced wall treatment, the turbulence models were modified in such a way as to allow the flow to be resolved all the way to the wall, that is, throughout the entire near-wall region.

#### 5. Results and Discussions

The distribution of static temperatures for a single 30°,60° and 90° holes is shown in the form of two-dimensional surface contours with the blowing ratios in 0.33 at bottom main flow surface downstream of the hole in figures 8 - 10. The direction of cross flow is from left to right, the origin of the axial distance x/D commence from the centre of the cooling hole. These contours shows that temperatures are decreasing on the two-dimensional surface with increasing blowing ratios due to these temperatures decreasing effectiveness of the film also decreasing on this surface.

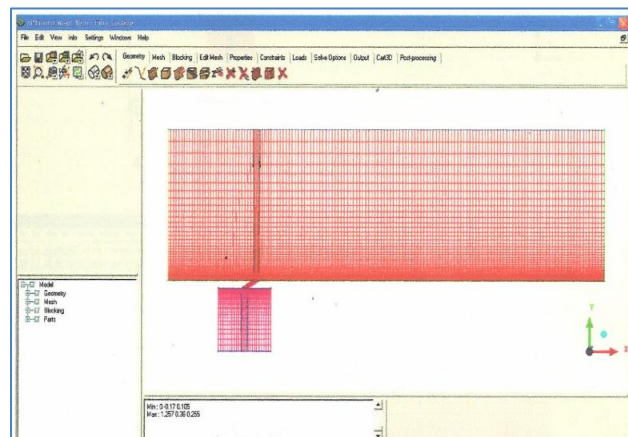


Fig 5: Mesh for 30 degree stream wise injection angle

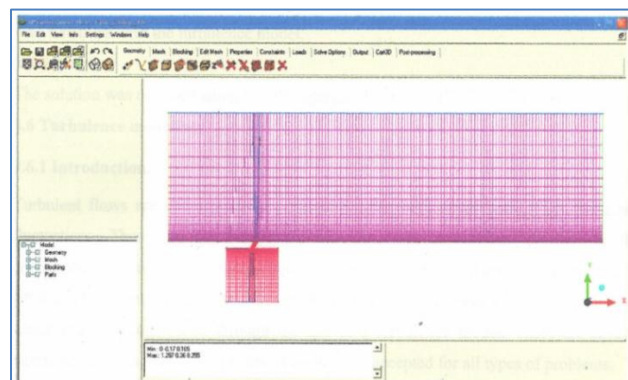
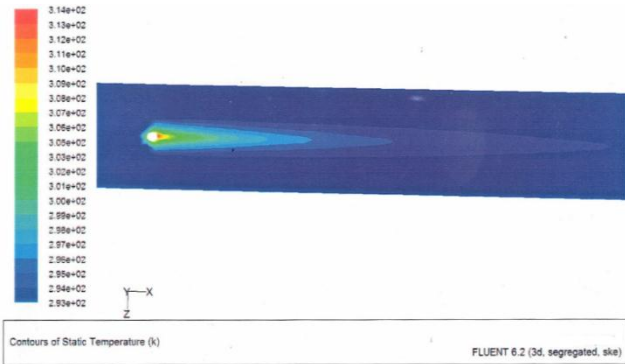


Fig 6: Mesh for 60 degree stream wise injection angle

In both meshes, boundary layer refinement at the top wall of the film coolant supply plenum, the bottom (measurement) wall of the main flow volume used. The goal of this was to give wall y+ values in these regions that would remove the requirement of using wall functions with the turbulence model.

With increasing blowing ratios the coolant spreads throughout the chamber and decreases the effectiveness on the surface.



**Fig 8:** Static temperature on the main flow bottom surface downstream of the film cooling hole ( $M=0.33, 30^\circ$ )

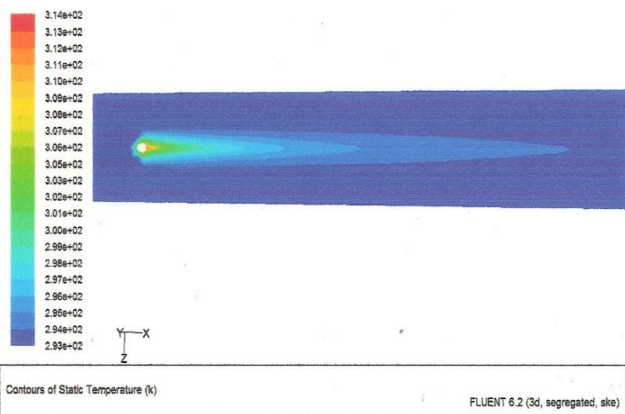


**Fig 9:** Static temperature on the main flow bottom surface downstream of the film cooling hole ( $M=0.33, 60^\circ$ )

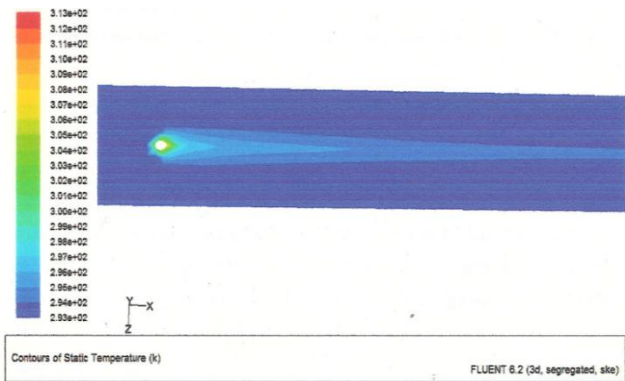


**Fig10:** Static temperature on the main flow bottom surface downstream of the film cooling hole ( $M=0.33, 90^\circ$ )

The static temperature contour shows the surface has less effectiveness due to increasing blowing ratio and stream wise injection angle  $90^\circ$ .

Figures 11 and 12 shows the vorticity contours near the hole region which is attached to the main flow bottom surface for  $M= 0.33$  with  $30^\circ$  and  $60^\circ$  injection angle. The temperature distribution on the down stream of the trailing

edge depends on this vorticity also. For increasing blowing ratios the vorticity is more near the hole region as shown in figures 11 and 12.

Figures 5.17 and 5.18 shows the vorticity contours for  $60^\circ$  injection angle in this case the vorticity is more in the case of  $M= 1.67$  compare to  $0.33$  . The vorticity intensity near the hole is more compare to the  $30^\circ$  injection angle case.

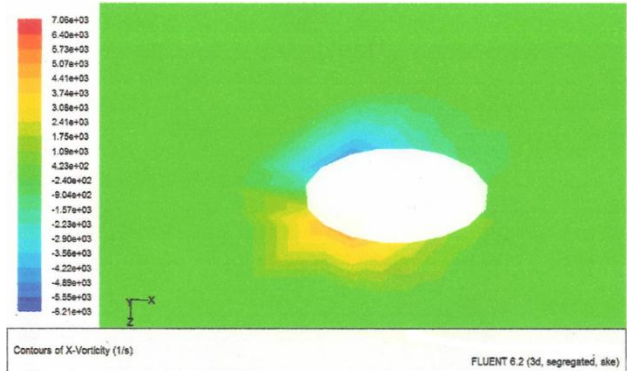


**Fig11:** Contours of axial component of vorticity ( $M=0.33, 30$  deg)

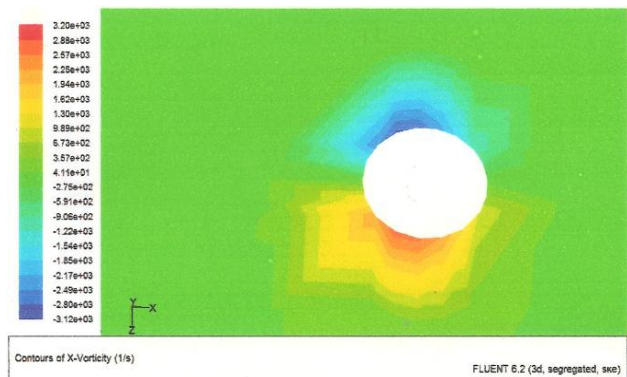


**Fig12:** Contours of axial component of vorticity ( $M=0.33, 60$  deg)

Figures 13 to 15 show the velocity vectors in the hole region for three stream wise injection angles for blowing ratios 0.33 and 1.67. These contours show the velocity vectors intensity is more at blowing ratio 1.67. but in this paper we show only for 0.33 blowing ratio even though my work was carried for blowing ratios 0.33 and 1.67.

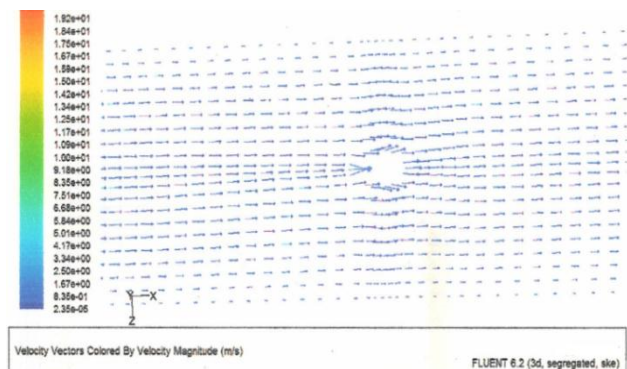


**Fig13:** Velocity vectors ( $M=0.33, 30$  deg)

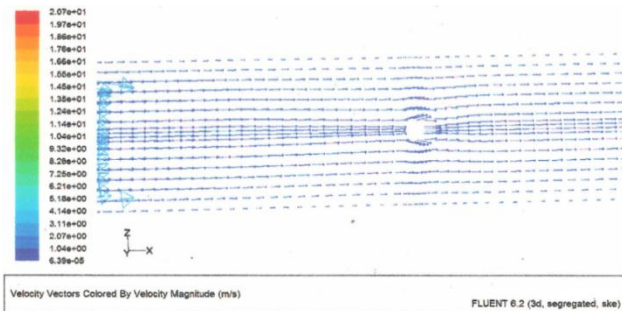


Fig14: Velocity vectors (M=0.33, 60 deg)

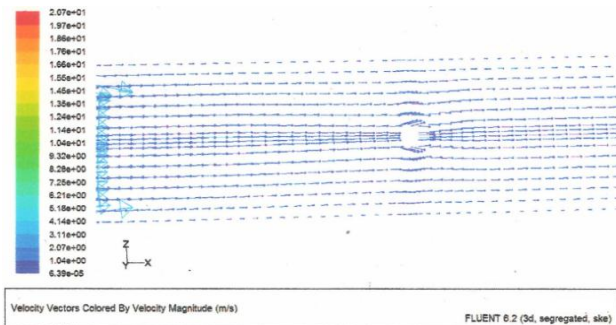


Fig15: Velocity vectors (M=0.33, 90 deg)

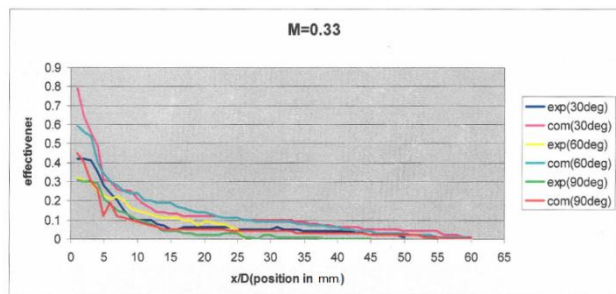


Fig 16: Comparison of centerline effectiveness versus non-dimensional position between three stream wise angles with experimental result. (M=0.33)

In the above fig.16 it shows the comparison of centerline effectiveness versus non-dimensional position between three stream wise angles with experimental results for the blowing ratio  $M=0.33$ . the maximum effectiveness achieved by the  $30^\circ$  jet in the immediate region with a blowing ratio  $M=0.33$  was higher than that by the steeper( $60^\circ$  and  $90^\circ$ )jets. This is due to the reason, the jet remained closest to the wall and with this blowing ratio the effectiveness is more on the main flow bottom surface. The effectiveness is more compared to experimental values.

The effectiveness achieved by the  $60^\circ$  stream wise angle is less compare to  $30^\circ$  stream wise injection angle because of the  $60^\circ$  jet was vertically further from the wall. The effectiveness achieved by the  $90^\circ$  jet was less than  $60^\circ$  and  $30^\circ$  jet, due to the  $90^\circ$ jet was furthest from the main flow bottom surface. The effectiveness achieved by the  $90^\circ$  jet was near to the experimental values compared to other 2 jets.

## Conclusions

In order to investigate the film cooling effectiveness at the downstream of the main flow bottom surface 3 stream wise angles and six blowing ratios are taken  $30^\circ$  stream wise injection angle shows greater effectiveness compare to the other 2 angles. Due to increased blowing ratios the effectiveness is decreased due to coolant is laterally distributed far downstream of the hole.  $30^\circ$  angle is near to the main flow bottom surface and the lateral distribution of more compare to  $60^\circ, 90^\circ$ . Since it was thought that vortex structure generated within the hole and downstream of the hole, the vortices immediately downstream of the hole were compared between the two stream wise injection angles. It was found that the more vortices intensity found near the hole region for increased blowing ratios. These vortices show effect on effectiveness. Due to increased vorticity the coolant spreads far downstream of the hole and reduces effectiveness on the surface.

## References

Yuen, C.H.N., and Martinez-Botas, R.F., (2003), Film Cooling Characteristics of a Single Round Hole at Various Streamwise Angles in a Crossflow: Part I Effectiveness, International Journal of Heat and Mass Transfer, Vol. 46, pp. 221-235.

Yuen, C.H.N., and Martinez-Botas, R.F., (2003), Film Cooling Characteristics of a Single Round Hole at Various Streamwise Angles in a Crossflow: Part II Heat Transfer Coefficients, International Journal of Heat and Mass Transfer, Vol. 46, pp. 237-249.

D. K. Walters and J. H. Lylek,( 1997) A Systematic Computational Methodology Applied to a Three-Dimensional Film-Cooling Flow field, ASME Journal of Turbomachinery, Vol 119, pp-777-785.

Brown, A., and Saluja, C.L., (1978), Film Cooling from a Single Hole and a Row of Holes of Variable Pitch to Diameter Ratio, International Journal of Heat and Mass Transfer, Vol. 22, pp. 525-533

R. S. Bunker, D. E. Metzger and S. Wittig, (1992) Local Heat Transfer in Turbine Disk Cavities: Part I—Rotor and Stator Cooling With Hub Injection of Coolant, ASME Journal of Turbomachinery, Vol.114, pp-211-220.

R. S. Bunker, D. E. Metzger and S. Wittig, (1992) Local Heat Transfer in Turbine Disk Cavities: Part II—Rotor Cooling With Radial Location Injection of Coolant, ASME Journal of Turbomachinery, Vol.114, pp-221-228.

D. L. Schmidt, B. Sen and D. G. Bogard (1996), Film Cooling With Compound Angle Holes: Adiabatic Effectiveness, ASME Journal of Turbomachinery, Vol.118, pp- 807-813.

G. E. Andrews, M. Alikhanizadeh, A. A. Asere, C. I. Hussain, M. S. Khoshkbar Azari and M. C. Mkpadi, (1986), Small Diameter Film Cooling Holes: Wall Convective Heat Transfer, Journal of Turbomachinery, Vol.108, pp-283-289.

D. Crabb, D. F. G. Durao and J. H. Whitelaw (1981), A Round Jet Normal to a Crossflow Journal of Fluids Engineering, Vol.103, pp-142-153.

Rhee, D.H., Lee, Y.S., Kim, Y.B., and Cho, H.H., (2003), Film Cooling and Thermal Field Measurements for Staggered Rows of Rectangular-Shaped Film Cooling Holes, ASME Paper No. GT2003-38608, Proceedings of ASME Turbo Expo 2003.

H.H. Cho, R.J.Goldstein, (1995), Heat (mass) transfer and film cooling effectiveness with injection through discrete holes: part I- within holes and on the back surface, Journal of Turbomachinery, Vol.117, pp-440-449.

Michael Glenn Durham, Comparison Of Square-Hole And Round-Hole Film Cooling: A Computational Study, A thesis submitted in partial fulfillment of the requirements for the degree of Master of Science, College of Engineering and Computer Science, Orlando, Florida, 2004.

Haven, B.A., and Kurosaka, M., (1997), Kidney and Anti-Kidney Vortices in Crossflow Jets, Journal of Fluid Mechanics, Vol. 352, pp. 27-64.

Baldauf, S., Schulz, A., and Wittig, S., (2001), High-Resolution Measurements of Local Effectiveness From Discrete Hole Film Cooling, ASME Journal of Turbomachinery, Vol. 123, pp. 758-765.

Ansys Manual.